

Are your **MRI contrast agents** cost-effective?

Learn more about generic **Gadolinium-Based Contrast Agents**.



**AJNR**

**Poststroke Cerebral Peduncular Atrophy  
Correlates with a Measure of Corticospinal  
Tract Injury in the Cerebral Hemisphere**

V.W. Mark, E. Taub, C. Perkins, L.V. Gauthier, G. Uswatte  
and J. Ogorek

This information is current as  
of April 20, 2024.

*AJNR Am J Neuroradiol* published online 16 November  
2007

<http://www.ajnr.org/content/early/2007/11/16/ajnr.A0811.citation>

ORIGINAL  
RESEARCH

V.W. Mark  
E. Taub  
C. Perkins  
L.V. Gauthier  
G. Uswatte  
J. Ogorek

# Poststroke Cerebral Peduncular Atrophy Correlates with a Measure of Corticospinal Tract Injury in the Cerebral Hemisphere

**BACKGROUND AND PURPOSE:** Methods have not been well developed and tested to predict the extent of remote degeneration in the central nervous system that follows cerebral infarction. We hypothesized that the extent of infarction overlap with the cerebral hemispheric course of the corticospinal tract (CST) on structural MR imaging predicts the extent of ipsilateral cerebral peduncular atrophy in patients with chronic stroke.

**MATERIALS AND METHODS:** Hemiparetic patients ( $n = 34$ ) with supratentorial unilateral infarctions who were at least 1 year poststroke onset and enrolled in research protocols of Constraint-Induced Movement therapy underwent volumetric T1 MR imaging of the brain. The following measures were calculated for each patient: 1) the maximal proportion of the CST in the cerebral hemisphere on axial section that was overlapped by infarction, 2) total infarction volume, and 3) the ratio of the cross-sectional area of the ipsilateral cerebral peduncle to the area of the contralateral cerebral peduncle (peduncular asymmetry ratio). Correlation analyses evaluated the predictive value of CST injury or infarction volume for the peduncular asymmetry ratio.

**RESULTS:** CST injury correlated significantly with the peduncular asymmetry ratio ( $r = -0.65$ ;  $P < .001$ ), whereas infarction volume did not ( $r = -0.31$ ;  $P = .09$ ).

**CONCLUSIONS:** The extent of postinfarction CST injury in the cerebral hemisphere predicts the extent of ipsilateral cerebral peduncular atrophy. More generally, the findings suggest that the extent of remote wallerian degeneration of a fiber tract is strongly related to its extent of injury directly at the site of infarction.

**M**R evaluations of acute focal ischemia (eg, diffusion-weighted imaging, adjusted diffusion coefficient mapping) made within only hours of stroke onset can predict the spatial extent of infarction months later.<sup>1-4</sup> In contrast, there has been little attempt to determine whether the size of the cerebrovascular lesion at any time can predict the degree of poststroke remote tissue loss in the central nervous system (CNS).

Anterograde volume loss after stroke can occur through either “wallerian” degeneration of the lesioned neurons or transsynaptic degeneration.<sup>5-7</sup> In either case, the volume loss does not become visible until at least several months poststroke.<sup>8-13</sup> The cerebral peduncle is ideal for assessing postinfarction wallerian degeneration, because its fibers (which are corticofugal) are completely arrayed in parallel, in contrast to most other brain stem areas.<sup>14,15</sup> The degree of peduncular atrophy from wallerian degeneration after supratentorial infarction can be conveniently expressed by dividing the peduncular area on the atrophied side by the area on the contralateral side at the same level in the axial plane.<sup>16,17</sup>

Neuroimaging studies in stroke only rarely examine structural pathologic changes beyond the first year after onset. We had the opportunity to examine whether structural MR imaging of chronic supratentorial infarction could predict the extent of concurrent ipsilateral peduncular atrophy.

Specifically, we assessed the extent of injury to the corticospinal tract (CST) in the cerebral hemisphere,<sup>18</sup> because the CST constitutes a sizable fraction of the total peduncular transaxial area (~25%),<sup>19</sup> and, therefore, CST degeneration could substantially affect the extent of postinfarction peduncular atrophy. The patients in our study were specifically recruited for mild-to-moderate chronic hemiparesis and, thus, were likely to have CST injury.<sup>20-23</sup> We hypothesized that in such patients the hemispheric extent of lesion to the CST would significantly correlate with the extent of cerebral peduncular atrophy and to a greater extent than would the volume of the infarction. Such a finding would suggest that a simple, predictable relationship exists between the amount of postinfarction structural injury at discrete and widely separated portions of the same fiber tract. The findings could benefit interpreting the clinical effects of chronic infarction in relation to associated tissue loss at different locations in the neuraxis.

## Materials and Methods

### Patients

Participants were adults who were enrolled to undergo Constraint-Induced Movement therapy (CI therapy) for chronic poststroke upper extremity hemiparesis<sup>24-27</sup> as part of several research investigations to evaluate the importance of various treatment factors for therapeutic outcomes. Because the therapy requires massed practice training with the more-affected arm on various tasks that involve active movement, patients with complete hemiplegia were excluded. The studies were approved by our institution’s review board for human research, and all of the patients provided signed informed consent. Patients were enrolled from 1997 to 2006.

Received March 26, 2007; accepted after revision July 30.

From the Departments of Physical Medicine and Rehabilitation (V.W.M.) and Psychology (E.T., C.P., L.V.G., G.U., J.O.), University of Alabama at Birmingham, Birmingham, Alabama.

This work was supported by grant HD34273 from the National Institutes of Health.

Please address correspondence to Victor W. Mark, Department of Physical Medicine and Rehabilitation, University of Alabama at Birmingham, 619 19th St South, SRC 190, Birmingham AL 35249-7330; e-mail: vmark@uab.edu

DOI 10.3174/ajnr.A0811

Patients included in the present study were required to have had volumetric T1-weighted brain MR imaging scans performed according to our project's criteria at our institution immediately preceding or during the 2- or 3-week treatment period. Clinical inclusion criteria for the research programs included the following: poststroke interval more than 12 months; average item score by the more-affected arm at or less than 2.5 (maximum possible score = 5) on the 30-item Motor Activity Log<sup>24,28</sup> (a validated self-report measure of real-world arm use<sup>29</sup>); general medical stability; and ability to follow directions from project therapists. Patients were enrolled regardless of age, hand preference, laterality of motor deficit, stroke etiology (eg, hemorrhagic versus nonhemorrhagic), and number of strokes. Patients were excluded from the present study if their infarctions were bilateral or occurred at or below the level of the cerebral peduncles. Patients were included regardless of whether they had solitary or multiple unilateral hemispheric infarctions, because we regarded all of the hemispheric infarctions as potential contributors to peduncular atrophy. All of the patients were required to have sufficient documentation from medical records and medical examination by project neurologists to determine that stroke had been the only cause for chronic hemiparesis.

From 52 patients who were originally recruited to participate in the clinical studies, 17 were excluded from the present study because of lesions at or below the cerebral peduncles or occupying both hemispheres within individual patients. The final sample of 34 patients (19 men) were, on average, 4.7 years ( $\pm 4.1$  years; range: 1–20 years) poststroke.

### MR Image Acquisition and Analysis

Imaging for this study depended on the availability of specific scanners at our institution, which varied over the years of this research program. Consequently, patients were evaluated on scanners that differed according to magnetic field strength and manufacturer. Thirteen patients were scanned on a 3T machine with the following parameters: whole-brain scan with approximately 130 sections of 1-mm thickness containing no gaps between sections, T1 turbo-field echo, TR = shortest, TE = 4.60 ms, matrix size =  $240 \times 240$  ms; reconstructed size =  $256 \times 256$  mm, voxel size =  $1.04 \times 1.05 \times 1.00$  mm<sup>3</sup>, FOV = 250, and flip angle = 8°. Ten patients were scanned on a 1.5T machine with the same parameters except for TR = 20 ms and TE = 6 ms. Eleven were scanned on a different 1.5T machine with the same parameters except for TR = 30 ms, TE = 6 ms, and flip angle = 45°. All of the scans were volumetric T1-weighted with axial scans set parallel to the orbital-meatal line. The images were stored in uncompressed Digital Imaging and Communications in Medicine format on the Clinical Image Management System archive developed by the computer-assisted neurosurgery facility at our institution.

MRICro version 1.4 (available at <http://www.sph.sc.edu/comd/rorden/mricro.html>) image analysis software was used for structural measurements. The images of 4 bilaterally symmetric and intact structures (eyes, optic chiasm, margins of the middle cranial fossa, and auditory canals) were used as references to correct the amount of roll (lateral tilt) within the axial images. The roll in the scans was manually adjusted until these 4 structures appeared by inspection to be symmetrically visible within their respective horizontal sections.

The peduncles were then measured with the method of Warabi et al.<sup>16</sup> The brightness level in MRICro was adjusted to ascertain that the margins of the midbrain were clearly visible. The axial level that showed the greatest expansion of the cerebral peduncles was identified on the MR imaging scans. The medial boundary of the cerebral peduncle was determined by connecting the oculomotor nerve sulcus

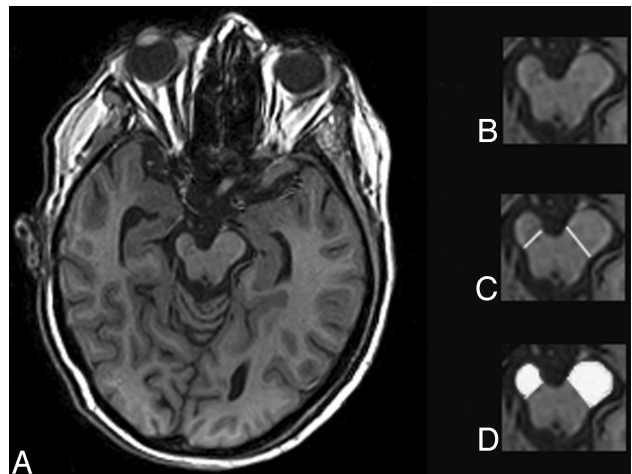


**Fig 1.** Determination of peduncular asymmetry ratio. *A*, Original axial T1 image. *B*, Cerebral peduncles in magnified view, demonstrating smaller area on the figure's left than on the right. *C*, Demarcation of medial boundary of peduncles. *D*, The enclosed areas of the demarcated peduncles that are to be measured by planimetry, shown in white. The peduncular asymmetry ratio is then calculated in this instance by dividing the left area by the right area.

to the lateral sulcus of the midbrain. The cross-sectional area of the resulting enclosed figure was measured on both sides (Fig 1). The peduncular asymmetry ratio was calculated by the peduncular area ipsilateral to the infarction divided by the peduncular area contralateral to the infarction. In our study, the method of peduncular asymmetry ratio calculation was highly reliable (intraclass correlation coefficient = 0.9).

Infarctions were traced in MRICro by researchers under the supervision of the project's current neurologist (V.W.M.) while blind to the clinical measures. Brightness levels were adjusted to maximally reveal the extent of suspected infarctions, which were defined as homogeneously hypointense regions of the parenchyma with distinct boundaries, of which the gray-scale values approximated those of the CSF within the lateral ventricles. (Chronic infarctions, unlike acute and subacute infarctions, have approximately the same T1 relaxation times as CSF.<sup>30</sup>) Parenchymal lucencies that were at or less than 0.2 cm across or that were either linear or round with a smooth margin were judged to represent perivascular spaces rather than infarctions<sup>31</sup> and, therefore, were not traced, except when no other lucencies were present that could account for hemiparesis. The total infarction volume was based on the sum of all of the individual unilateral hemispheric infarctions. In our sample, 24 patients had single infarctions, and 10 patients had multiple unilateral infarctions.

The technique that was used to measure the maximal amount of postinfarction injury to the CST in the cerebral hemisphere was described by Pineiro et al.<sup>18</sup> An infarction mask was initially created on each patient's scan by manually tracing each infarction within its corresponding horizontal section. The CST mask was then created by transferring to the MR image the boundaries of the CST that were indicated on the axial views from the Talairach atlas<sup>32</sup> at approximately the same anatomic levels as those of the infarction. The area of the infarction and the area of the CST, as identified by the Talairach atlas, were then outlined within each horizontal section that contained both, and the proportion of the CST area in which the 2 masks overlapped was calculated with planimetry. This process was applied to each section of the MR imaging that demonstrated infarction. The largest proportional amount of CST area overlap by infarction among all of the MR imaging sections showing overlap was identified and

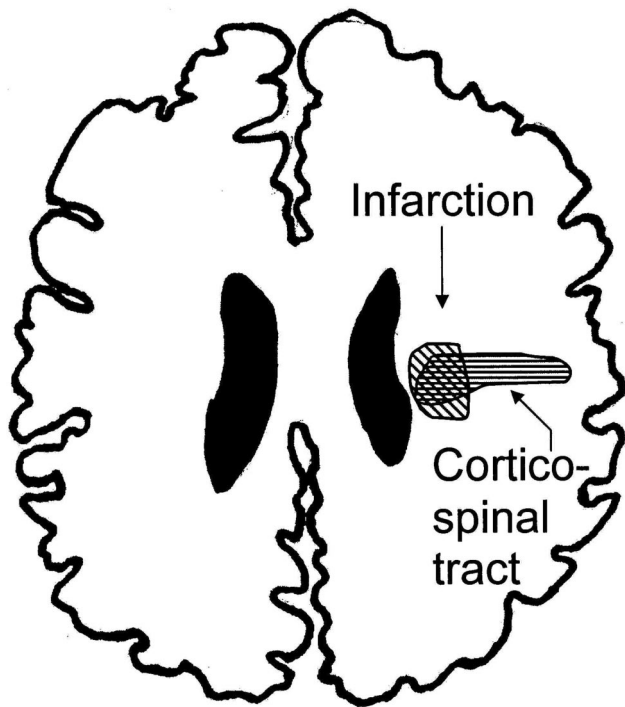


**Fig 2.** Schematic demonstration of calculation of maximal proportional CST overlap by infarction. In this example, the infarction overlaps 30% of the CST area in the axial plane.

used to index the amount of CST damage (Fig 2). The resulting measure could range from 0%, indicating no overlap between the masks, to 100%, indicating complete overlap of the CST mask by the infarction mask.

### Statistical Analysis

Pearson correlation analyses were used to identify any possible relationship between the amount of peduncle asymmetry and the percentage of overlap of the CST mask by the infarction mask and also to determine whether total infarction volume was related to peduncular asymmetry. Significance level was set to  $P < .05$ .

### Results

#### Neuroimaging Findings

The peduncular area ipsilateral to the infarction(s) was, on average, 72% of the peduncular area contralateral to the infarction(s). The average percentage of maximal CST overlap by infarction was 49%. Average total infarction volume was 19 cm<sup>3</sup> (range, 0.04–157.00 cm<sup>3</sup>). There was no interaction between the specific scanner used and the associated infarction volumes ( $F_{2,32} = 0.992$ ;  $P = .38$ ), which suggests that the scanners were comparable in their sensitivity to and resolution of cerebral infarctions, despite differences in magnetic field strength.

#### Correlation between Peduncle Asymmetry and CST Damage

The peduncular asymmetry ratio was significantly related to the amount of infarction overlap with the CST ( $r = -0.65$ ;  $P < .001$ ; Fig 3). This finding provided preliminary support for the hypothesis that the extent of CST injury in the cerebral hemisphere is correlated with the extent of peduncular atro-

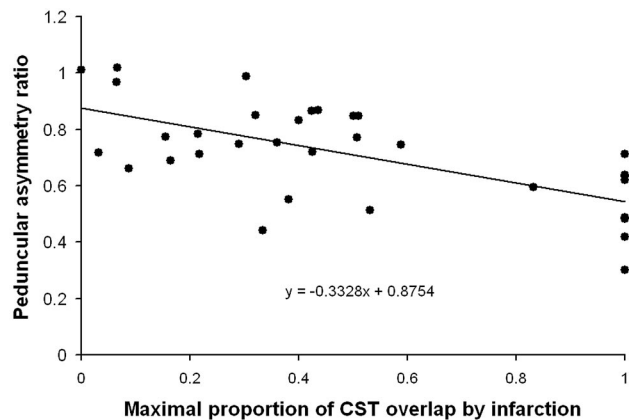


**Fig 3.** Relationship between peduncular asymmetry ratio and maximal proportion of CST overlap by infarction in the cerebral hemisphere.

phy. However, whereas the CST-infarction overlap method directly assesses CST injury, peduncular asymmetry is not specific to CST injury, because other corticofugal tracts also traverse the peduncles other than the CST (ie, frontopontine, temporopontine, parietopontine, and occipitopontine fibers).<sup>19,33</sup> Consequently, extensive cerebral injury outside of the CST could have disproportionately affected peduncular asymmetry by damaging these other fibers, thus possibly affecting our ability to detect an effect from CST injury alone. We, therefore, reexamined the correlation between the peduncular asymmetry ratio and the proportional extent of overlap with the CST by excluding patients with the largest infarction volumes. However, excluding patients whose total infarction volumes were greater than 2 SDs from the mean (ie, 30 cm<sup>3</sup>;  $n = 9$ ) did not change the significance of the relationship between CST injury and peduncular asymmetry ( $r = -0.51$ ;  $P = .01$ ). The correlation between peduncle asymmetry and total infarction volume was weak and not significant ( $r = -0.31$ ;  $P = .09$ ).

### Discussion

Our findings indicate that the calculated maximal proportion of CST overlap by cerebral infarction was superior to total infarction volume for predicting the extent of ipsilateral peduncular atrophy on axial imaging sections in patients with chronic poststroke hemiparesis, at least for subjects who qualified for CI therapy. Previous research for the most part has not evaluated whether the extent of vascular lesion at any stage can predict the extent of remote tissue loss. The one exception was Khong et al,<sup>34</sup> who evaluated 11 hemiparetic children at least 1 year after middle cerebral artery infarction. Their study's atrophy ratio, based on comparing left and right sides of the midbrain rather than the peduncles, was significantly correlated with the maximum area of infarction in the hemisphere as seen on axial views ( $r = -0.70$ ). Although Khong et al<sup>34</sup> used different methods than we did, their findings similarly suggest that the planar extent of supratentorial infarction is directly related to the amount of postinfarct degeneration along the corticofugal fibers of the midbrain. Our findings furthermore show that it is the areal extent of infarction, and not its volumetric extent, that determines the amount of remote tissue loss along a tract. This implies that there is a lawful relationship between the 2D extent of an infarction that ex-



tends perpendicularly through a fiber bundle and the areal loss along the same fiber bundle remotely.

It is unclear whether our findings would generalize to all stroke patients with chronic hemiparesis, because we used strict clinical inclusion criteria. However, the mean total infarction volume and volume ranges in our sample did not differ markedly from infarction volumes reported in acute stroke surveys with broader inclusion criteria.<sup>2,3,35-37</sup> Consequently, it is unlikely that our clinical inclusion criteria would strongly alter the relationships that would be obtained between infarction measures and peduncular atrophy for chronic hemiparetic stroke patients in general.

A methodologic limitation of our study was its use of the CST representation as depicted in the Talairach atlas. The cortical extent of the CST representation in the atlas extends only to Brodmann area 4 (the precentral gyrus), whereas the CST actually originates from more widely distributed cortical areas.<sup>19</sup> However, this restriction in the depiction of the origin of the CST did not prevent our uncovering a significant and biologically plausible relationship between the amount of CST injury at the site of infarction and the extent of remote ipsilateral atrophy in the peduncle.

The atrophic changes in the cerebral peduncles that followed supratentorial infarction reflected the effects of wallerian degeneration rather than transsynaptic degeneration, because the peduncles consist only of corticofugal fibers that originate from the ipsilateral hemisphere and do not include cell bodies. Among stroke patients with chronic hemiparesis, wallerian degeneration of the CST would be expected to significantly account for the variance in the cross-sectional area of the atrophied cerebral peduncle, though other corticofugal fibers in the peduncle could also have degenerated after supratentorial infarction. Our findings suggest that, as a general principle, the areal extent of remote wallerian degeneration of a fiber tract is proportional to the maximal proportional extent of the infarction's overlap with a planar representation of the unlesioned boundary of the involved fiber bundle, because axonal injury close to the origin of the tract should occur in an anterograde manner throughout the remainder of the tract. The CST is well defined at multiple levels of the neuraxis and, therefore, readily lends itself to such evaluation. Such a relationship would probably be less strong in CNS regions in which the fibers course bidirectionally (eg, corpus callosum), have diverse spatial orientations (eg, pons), or may be difficult to image due to technical constraints (eg, spinal cord), but nonetheless the extent of infarction overlap with a particular fiber bundle should be consistently related to the resulting atrophy at other, remote portions of the same tract. Further research that would use diffusion tensor imaging might confirm this hypothesis due to its ability to specify more precisely the course of fiber bundles within individual patients, as opposed to transposing from a generic brain atlas, as we have done here.

It should be noted, however, that not all diseases that lesion the CST behave in this manner. In particular, amyotrophic lateral sclerosis and corticobasal degeneration have been shown to be associated with selective atrophy of the CST in the medulla but not the midbrain, despite the loss of Betz cells in the motor cortex.<sup>38,39</sup> These findings suggest that retrograde degeneration of the CST occurs in neurodegenerative disor-

ders, which is absent after supratentorial cerebral infarction. Consequently, considerably different neuropathologic mechanisms appear to govern CST atrophy in various cerebral motor neuron disorders.

Our findings help to provide a more comprehensive understanding of the clinical-pathologic relationships that follow stroke. The significant relationship that has been demonstrated to occur between acute ischemic lesion extent and infarction extent later in the first year after stroke onset ( $r_s = 0.68-0.84$ )<sup>1,2</sup> suggests that the acute ischemic lesion extent could also reliably predict the amount of subsequent post-stroke loss in the remote CST due to wallerian degeneration, at least in the affected cerebral peduncle. Our findings also suggest that the significant relationship between infarction extent in chronic stroke and concurrent motor findings<sup>18,21</sup> may be entirely due to local infarction effects and is not additionally affected by the extent of remote tissue loss.

## Conclusion

Months are required before the associated wallerian degeneration after cerebral infarction effects appreciable volume loss. Within a sample of hemiparetic chronic stroke patients, we found that a simple measure of the infarction's injury to the hemispheric course of the CST predicted the extent of remote tissue loss in the ipsilateral cerebral peduncle, which was likely to have resulted primarily from wallerian degeneration of the CST. We suggest that, in general, the extent of postinfarction tract necrosis close to the origin of a specific fiber tract has a predictable quantitative effect on anterograde tract atrophy remote from the site of injury.

## Acknowledgments

Andrew Timberlake is thanked for his contributions to data measurement and analysis.

## References

1. Lövsblad KO, Baird AE, Schlaug G, et al. Ischemic lesion volumes in acute stroke by diffusion-weighted magnetic resonance imaging correlate with clinical outcome. *Ann Neurol* 1997;42:164-70
2. Rivers CS, Wardlaw JM, Armitage PA, et al. Do acute diffusion- and perfusion-weighted MRI lesions identify final infarct volume in ischemic stroke? *Stroke* 2006;37:98-104
3. Barber PA, Darby DG, Desmond PM, et al. Prediction of stroke outcome with echoplanar perfusion- and diffusion-weighted MRI. *Neurology* 1998;51:418-26
4. Desmond PM, Lovell AC, Rawlinson AA, et al. The value of apparent diffusion coefficient maps in early cerebral ischemia. *AJNR Am J Neuroradiol* 2001;22:1260-67
5. Inagaki M, Koeda T, Takeshita K. Prognosis and MRI after ischemic stroke of the basal ganglia. *Pediatr Neurol* 1992;8:104-08
6. Rabin BM, Hebel DJ, Salamon-Murayama N, et al. Distal neuronal degeneration caused by intracranial lesions. *AJR Am J Roentgenol* 1998;171:95-102
7. Yamada K, Patel U, Shrier DA, et al. MR imaging of CNS tractopathy: wallerian and transneuronal degeneration. *AJR Am J Roentgenol* 1998;171:813-18
8. Kuhn MJ, Mikulis DJ, Ayoub DM, et al. Wallerian degeneration after cerebral infarction: evaluation with sequential MR imaging. *Radiology* 1989;172:179-82
9. Inoue Y, Matsumura Y, Fukuda T, et al. MR imaging of wallerian degeneration in the brain stem: temporal relationships. *AJNR Am J Neuroradiol* 1990;11:897-902
10. Hurwitz TA, Mandat T, Forster B, et al. Tract identification by novel MRI signal changes following stereotactic anterior capsulotomy. *Stereotact Funct Neurosurg* 2006;84:228-35
11. Giroud M, Fayolle H, Martin D, et al. Late thalamic atrophy in infarction of the middle cerebral artery territory in neonates. A prospective clinical and radiological study in four children. *Childs Nerv Syst* 1995;11:133-36
12. Kraemer M, Schormann T, Hagemann G, et al. Delayed shrinkage of the brain after ischemic stroke: preliminary observations with voxel-guided morphometry. *J Neuroimaging* 2004;14:265-72

13. Uchino A, Imada H, Ohno M. **MR imaging of wallerian degeneration in the human brain stem after ictus.** *Neuroradiology* 1990;32:191–95
14. Virta A, Barnett A, Pierpaoli C. **Visualizing and characterizing white matter fiber structure and architecture in the human pyramidal tract using diffusion tensor MRI.** *Magn Reson Imaging* 1999;17:1121–33
15. Pierpaoli C, Barnett A, Pajevic S, et al. **Water diffusion changes in wallerian degeneration and their dependence on white matter architecture.** *Neuroimage* 2001;13:1174–85
16. Warabi T, Miyasaka K, Inoue K, et al. **Computed tomographic studies of the basis pedunculi in chronic hemiplegic patients: topographic correlation between cerebral lesion and midbrain shrinkage.** *Neuroradiology* 1987;29:409–15
17. Warabi T, Inoue K, Noda H, et al. **Recovery of voluntary movement in hemiplegic patients.** *Brain* 1990;113:177–89
18. Pineiro R, Pendlebury ST, Smith S, et al. **Relating MRI changes to motor deficit after ischemic stroke by segmentation of functional motor pathways.** *Stroke* 2000;31:672–79
19. Carpenter MB. *Core Text of Neuroanatomy*, 3rd ed. Baltimore: Williams and Wilkins; 1985
20. Watanabe H, Tashiro K. **Brunnstrom stage and wallerian degenerations. A study using MRI.** *Tohoku J Exp Med* 1992;166:471–73
21. Bouza H, Dubowitz LM, Rutherford M, et al. **Prediction of outcome in children with congenital hemiplegia: a magnetic resonance imaging study.** *Neuropediatrics* 1994;25:60–66
22. Mazumdar A, Mukherjee P, Miller JH, et al. **Diffusion-weighted imaging of acute corticospinal tract injury preceding wallerian degeneration in the maturing human brain.** *AJNR Am J Neuroradiol* 2003;24:1057–66
23. Feydy A, Carlier R, Roby-Brami A, et al. **Longitudinal study of motor recovery after stroke: recruitment and focusing of brain activation.** *Stroke* 2002;33:1610–17
24. Taub E, Miller NE, Novack TA, et al. **Technique to improve chronic motor deficit after stroke.** *Arch Phys Med Rehabil* 1993;74:347–54
25. Mark VW, Taub E. **Constraint-induced movement therapy for chronic stroke hemiparesis and other disabilities.** *Restor Neurol Neurosci* 2004;22:317–36
26. Taub E, Lum PS, Hardin P, et al. **AutoCITE: automated delivery of CI therapy with reduced supervision from therapists.** *Stroke* 2005;36:1301–04
27. Wolf SL, Winstein CJ, Miller JP, et al. **Effect of constraint-induced movement therapy on upper extremity function 3 to 9 months after stroke: the EXCITE Randomized Clinical Trial.** *JAMA* 2006;296:2095–104
28. Taub E, Uswatte G, King DK, et al. **A placebo controlled trial of Constraint-Induced Movement therapy for upper extremity after stroke.** *Stroke* 2006;37:1045–49
29. Uswatte G, Taub E, Morris D, et al. **The Motor Activity Log-28: assessing daily use of the hemiparetic arm after stroke.** *Neurology* 2006;67:1189–94
30. Lundbom N, Katevuo K, Komu M, et al. **T1 in subacute and chronic brain infarctions. Time-dependent development.** *Invest Radiol* 1992;27:673–80
31. Bokura H, Kobayashi S, Yamaguchi S. **Distinguishing silent lacunar infarction from enlarged Virchow-Robin spaces: a magnetic resonance imaging and pathological study.** *J Neurol* 1998;245:116–22
32. Talairach J, Tournoux P. *Co-planar Stereotaxic Atlas of the Human Brain: 3-Dimensional Proportional System—An Approach to Cerebral Imaging.* New York: Thieme Medical Publishers; 1988
33. Abbie AA. **The projection of the forebrain on the pons and cerebellum.** *Proc R Soc Lond B* 1934;115:504–22
34. Khong PL, Zhou LJ, Ooi GC, et al. **The evaluation of wallerian degeneration in chronic paediatric middle cerebral artery infarction using diffusion tensor MR imaging.** *Cerebrovasc Dis* 2004;18:240–47
35. Lindgren A, Norrving B, Rudling O, et al. **Comparison of clinical and neuro-radiological findings in first-ever stroke. A population-based study.** *Stroke* 1994;25:1371–77
36. Beaulieu C, de Crespigny A, Tong DC, et al. **Longitudinal magnetic resonance imaging study of perfusion and diffusion in stroke: evolution of lesion volume and correlation with clinical outcome.** *Ann Neurol* 1999;46:568–78
37. Kissela B, Broderick J, Woo D, et al. **Greater Cincinnati/Northern Kentucky Stroke Study: volume of first-ever ischemic stroke among blacks in a population-based study.** *Stroke* 2001;32:1285–90
38. Tsuchiya K, Ikeda K, Mimura M, et al. **Constant involvement of the Betz cells and pyramidal tract in amyotrophic lateral sclerosis with dementia: a clinicopathological study of eight autopsy cases.** *Acta Neuropathol (Berl)* 2002;104:249–59
39. Tsuchiya K, Murayama S, Mitani K, et al. **Constant and severe involvement of Betz cells in corticobasal degeneration is not consistent with pyramidal signs: a clinicopathological study of ten autopsy cases.** *Acta Neuropathol (Berl)* 2005;109:353–66